ELSEVIER

Journal of Power Sources 109 (2002) 483–493

JOURNAL OF POWER SOURCES

www.elsevier.com/locate/jpowsour

A sharp peak in the performance of sputtered platinum fuel cells at ultra-low platinum loading

Ryan O'Hayre*, Sang-Joon Lee, Suk-Won Cha, Fritz. B. Prinz

Stanford University Rapid Prototyping Laboratory, Building 530, Room 226, Duena Street and Escondido Mall, Stanford, CA 94305, USA

Received 14 February 2002; accepted 7 March 2002

Abstract

Proton exchange membrane fuel cells were fabricated by direct sputter deposition of platinum on the surface of Nafion 117 membranes. A sharp spike in the performance of these sputtered platinum fuel cells was observed at ultra-low platinum thickness values of 5–10 nm. Within this narrow thickness range, the power output capability of sputtered platinum fuel cells is several orders of magnitude better than the performance produced by thinner or thicker coatings. The spike in performance is explained by rapid changes in the sputtered film microstructure at the nanometer thickness level. When the membrane surface is deliberately modified by abrasion prior to sputtering, this sharp peak is not seen. Instead, a broad plateau is observed, where the performance is insensitive to the amount of sputtered platinum. This behavior stems from how surface roughening affects the sputtered catalyst layer continuity. The performance of a sputter-deposited membrane with a platinum loading level of 0.04 mg/cm^2 is compared to a commercial membrane electrode assembly (MEA) with a platinum loading of 0.4 mg/cm^2. The maximum power output of the sputtered cell is three-fifths that of the commercial MEA, but uses one-tenth the platinum.

Keywords: Proton exchange membrane (PEM) fuel cells; Sputter deposition; Catalyst; Thin film

1. Introduction

Proton exchange membrane (PEM) fuel cells are particularly well suited for transportation and portable electronic power applications due to their good energy conversion efficiency and the high power density of their fuel sources [1]. To make PEM fuel cells a commercial reality, much development work in the past decades has focused on the performance improvement of polymer electrolytes, electro-catalysts, and electrode materials [2,3]. One important thrust of present research is lowering overall fuel cell costs [4]. Cost savings can be gained through several approaches, such as reducing electro-catalyst loadings or simplifying the cell design and manufacturing process.

Recently, several researchers have examined the sputter deposition technique as a means to reduce cell costs by achieving ultra-low levels of catalyst loading [5–7]. A 5 nm sputtered platinum film corresponds to a catalyst loading level of 0.014 mg/cm^2. In comparison, conventional cells have a platinum loading level around 0.4 mg/cm^2. Large area sputter deposition processes have been developed for the window glass industry, and are cost competitive with other coating technologies. Sputter deposition of catalyst can also simplify cell fabrication, leading to manufacturing cost reductions. Additionally, the sputter process is compatible with other integrated circuit (IC) fabrication technologies, rendering it ideal for micro-fuel cell applications [8]. Whereas conventional membrane electrode assemblies (MEAs) rely on a series of catalyst ink spraying or painting steps in combination with hot-pressing procedures to bond disparate carbon cloth electrodes to an electrolytic membrane [9], sputter-deposited cells are entirely thin film and require no additional preparation steps. While some catalyst wastage may occur in a sputter process, this is also true of a catalyst ink-based process. Furthermore, precious metals recovery and recycling techniques are routinely implemented in high volume commercial sputter deposition processes. The ability to sequentially sputter deposit both a catalyst film and an overlying porous or patterned current collector is a future goal. Sequential sputter deposition of both the catalyst and electrode would allow for a thinner, simplified fuel cell that is also 'configurable'; thus by changing the catalyst and electrode patterning, an assortment of fuel cell structures could be wired in various sizes and combinations to deliver, in essence, a 'designer' power source on a chip.

* Corresponding author. Tel.: +1-650-725-9936.
E-mail addresses: rohayre@stanford.edu (R. O'Hayre), sjlee@stanford.edu (S.-J. Lee), swcha@stanford.edu (S.-W. Cha), fprinz@stanford.edu (F.B. Prinz).

0378-7753/02/$ – see front matter
PII: S0378-7753(02)00238-0

To attain good performance, a sputter-deposited catalyst layer must satisfy the following requirements. First, it should maximize the available amount of three-phase zone, where the gas reactants, proton conducting phase, and the catalytically active electrically conductive phase are all present together. Second, it should be thin so as to minimize gas diffusion losses and aid in water removal. Third, the catalyst layer should adhere strongly to the membrane in order to reduce ohmic losses and to support the high mechanical stresses produced during operation. Since state-of-the-art powder supported catalyst layers contain platinum particles in the 10 nm range [10], sputtering techniques need to provide platinum domains of a comparable size or smaller in order to be competitive. A unique advantage of the direct sputtering technique is that the catalyst deposit is highly localized directly at the membrane interface. This results in an extremely high platinum utilization, which somewhat compensates for the ultra-low loading levels.

This work extends prior efforts on catalyst sputter deposition by examining in detail the effect of sputtered film thickness and morphology on fuel cell performance. It will be seen that fuel cell performance varies over several orders of magnitude depending on the thickness of the sputtered catalyst film. The possible reasons for this dramatic variation will be examined in detail, and are related to changes in the sputtered film microstructure. Cell polarization, electrochemical impedance spectroscopy (EIS), and cyclic voltammetry (CV) measurements are coupled with various microscopy techniques to elucidate the connection between the sputtered platinum microstructure and ultimate fuel cell performance. Intentional surface roughening of the polymer electrolyte membrane prior to catalyst sputter deposition will be investigated as a means to improve performance.

2. Experimental

2.1. Membrane and electrode assembly preparation

In order to provide a reduced system for quantitative study, the thin film platinum MEAs used in this study were made as simple as possible. They consisted only of ultra-thin sputtered platinum films deposited directly onto Nafion membranes. No carbon inks, binding materials, Nafion solutions, or other agents were used in their construction. This provided a well-defined membrane–catalyst interface.

Nafion 117 from ElectroChem Inc., was used in all experiments unless noted otherwise. In order to determine if prior roughening of the membrane surface had an effect on fuel cell performance, three different surface treatments of the Nafion membrane were investigated. Two degrees of roughened Nafion were first prepared by SiC abrasion for 30 s on a circular grinding wheel. Although, there are more elegant ways to induce surface roughness [11–13], SiC abrasion was chosen in light of its convenience and cost effectiveness. 'Fine roughening' was achieved by abrading the Nafion with 600-grit SiC sandpaper, while 'coarse roughening' was achieved by abrading Nafion with 400-grit SiC. Smooth Nafion was used as purchased, and not subjected to any roughening treatment. All three types of Nafion; smooth, fine roughened, and coarse roughened Nafion, were activated prior to platinum sputtering according to the following 6 h treatment routine:

- 1 h in DI water at 80 °C;
- 1 h in 30% H_2O_2 at 80 °C;
- 1 h in 85% H_2SO_4 at 80 °C;
- 1 h in DI water at 80 °C;
- 1 h in DI water at 80 °C;
- 1 h in DI water at 80 °C.

After activation, Nafion samples were sputtered through shadow masks to define 5 cm^2 active regions on both sides of each membrane. The samples were taken out of the vacuum chamber, exposed to ambient atmosphere, flipped, and then returned to vacuum to sputter the second side. The deposited platinum thickness was controlled by the sputtering time. Sputter conditions were 100 W and 30 sccm Argon at 0.67 Pa, resulting in a sputter deposition rate of approximately 1 nm/s. Sputtered MEA samples were prepared from all three types of Nafion, with nominal platinum film thickness ranging between 2 and 1000 nm.

2.2. Cell polarization measurements and electrochemical impedance spectroscopy

All fuel cell polarization measurements were conducted at room temperature using dry hydrogen and dry oxygen gas at 1 atm pressure. These modest conditions were used to mimic the environment most likely experienced by a passive micro-fuel cell device. The home built test fixture shown in Fig. 1 was used for all of the fuel cell testing. This test fixture used machined copper flow structures with a serpentine flow pattern, accommodating the 5 cm^2 single cell geometry that was standard for all of the MEAs tested. Carbon cloth electrodes were used in the fuel cell test fixture to assure proper electrical contact between the platinum sputtered Nafion membranes and the copper gas flow plates; however, these carbon cloth electrodes were not hot-pressed or in any other way fixed to the platinum coated Nafion membranes. Gas flow rates were regulated at 10 ml/min, and measurements were acquired via a Gamry PC4/750 potentiostat system linked to a PC.

EIS was conducted under the same cell polarization measurement conditions. A sinusoidal excitation signal with a 10 mV amplitude was used to investigate a range of frequencies from 100 kHz to 10 mHz at various cell potentials. The anode was used as the reference electrode.

2.3. Cyclic voltammetry

In situ CV was conducted using the same PC controlled Gamry PC4/750 potentiostat system, with Ar gas passing through the cathode (working electrode) and H_2 gas through

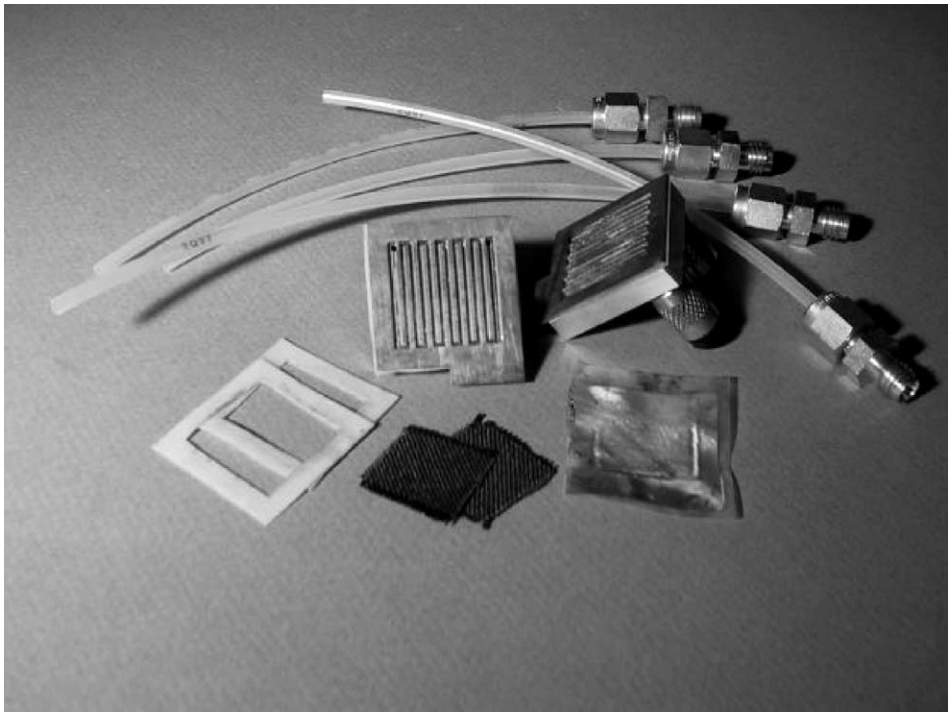

Fig. 1. Photograph of the fuel cell test fixture used for all electrochemical experimentation in this report. The fixture employs machined copper flow fields with serpentine channels, accommodating a 5 cm^2 single cell geometry.

the anode (counter electrode) at room temperature and 1 atm. To ensure a large counter electrode compared to the working electrode, the anode electrode area was maintained at 5 cm^2, while the cathode electrode area was reduced to 1 cm^2. Voltammograms were obtained at a scan rate of 40 mV/s with the potential cycled between −0.1 and +1.0 V. Flow rates for both gases were fixed at 10 ml/min. The counter electrode also served as the reference electrode due to its negligible overpotential. Active platinum surface area was obtained by measuring the charge (Q_h) required for hydrogen desorption from the platinum surface after excluding double layer charge effects. An active platinum area coefficient (A_c) was calculated which represents the ratio of the measured active platinum surface area compared to the active platinum surface area of an atomically smooth platinum electrode of the same size. A highly irregular platinum electrode may have an active surface area that is orders of magnitude larger than its geometric area. This effect is expressed through A_c. The monolayer absorption charge (Q_m) for atomically smooth platinum was taken as 210 μC/cm^2.

$$A_c = \frac{\text{measured electrically active platinum surface area}}{\text{geometric surface area}} = \frac{A_{active}}{A_{geometric}} = \frac{Q_h}{Q_m A_{geometric}}$$

2.4. Microscopy

AFM studies of the platinum sputtered membranes were performed in air under normal atmospheric conditions using a Digital Instruments NanoScope III scanning probe microscope. Imaging was performed in contact mode using a scanner with maximum x, y, z translations of 120 μm × 120 μm × 5 μm. AFM images of platinum films on roughened Nafion membranes could not be obtained owing to limitations in the z-range of the scanner. Standard silicon nitride tips with a force constant of 0.06 N/m were used. Images were plane-fit leveled; quantitative data were extracted from the leveled images using the accompanying digital instruments NanoScope™ III analysis package.

Additional microscopy of both the smooth and rough platinum coated membranes was performed using a Polyvar MET optical microscope and a Hitatchi S-2500 scanning electron microscope (SEM).

3. Results and discussion

3.1. The effect of platinum film thickness on fuel cell performance

The performance of sputtered platinum fuel cells depends strongly on the thickness of the sputtered catalyst layer. While platinum can be sputtered onto Nafion membranes in films up to several microns thick, it was found that films only 5–10 nm thick produce the best fuel cell performance. These ultra-thin films not only optimize performance, but also result in ultra-low platinum loading levels in the 0.01–0.02 mg/cm^2 range. It was unexpected that such thin platinum coatings (barely even visible to the naked eye) could deliver good performance.

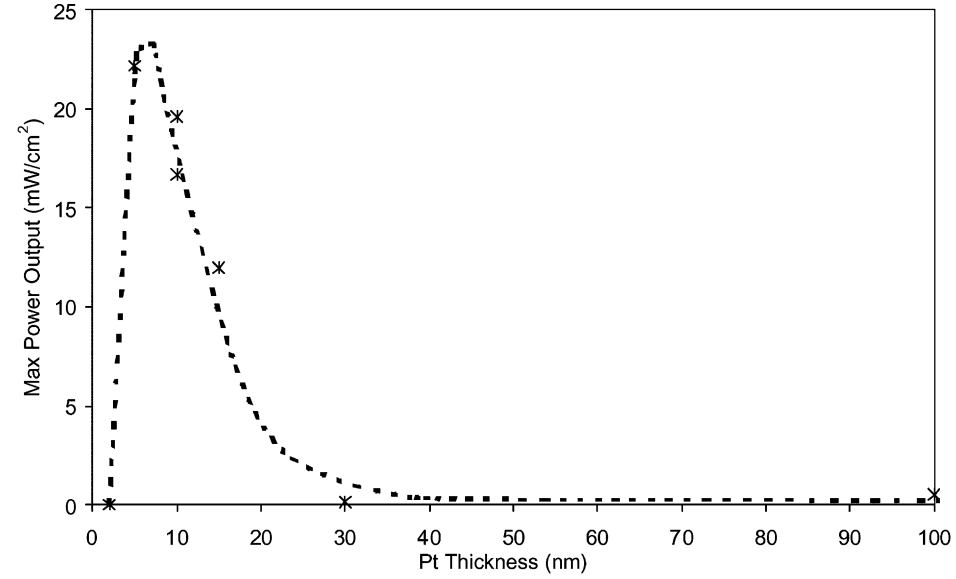

(a)

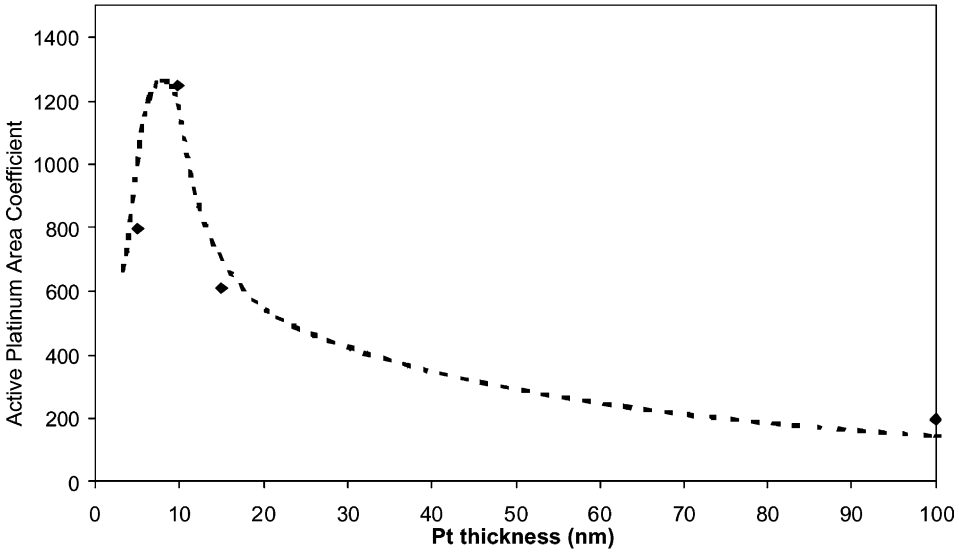

(b)

Fig. 2. (a) Fuel cell performance vs. platinum thickness for smooth Nafion 117 sputter-coated membranes, (b) active platinum area vs. platinum thickness for smooth Nafion 117 sputter-coated membranes. Electrochemical measurements were taken at room temperature using dry (non-humidified) H_2/O_2 at 1 atm.

In Fig. 2a, the performance of smooth Nafion membranes catalyzed by sputter-deposited platinum is charted versus platinum film thickness. Performance of the sputtered cells was characterized in terms of the maximum power density attained by a cell during standard polarization measurement. Fuel cell performance exhibits a sharp peak around 5–10 nm of platinum thickness, with maximum power dropping off appreciably for platinum films that are thicker or thinner. A CV study of the platinum sputtered membranes further corroborates this narrow performance peak at ultra-low sputtered platinum thickness. As shown in Fig. 2b, active platinum area also reaches a maximum in the 5 nm thickness regime before declining with increasing sputtered film thickness. These dramatic changes in performance and catalytic behavior suggest a rapidly evolving platinum film microstructure at the nanometer thickness level.

3.2. Microscopy investigation of sputtered platinum

While a peak in performance was expected in an abstract way, the sharpness and narrowness of the peak, as well as its location at ultra-low platinum thickness, was not expected. In order to understand how thickness variations at the

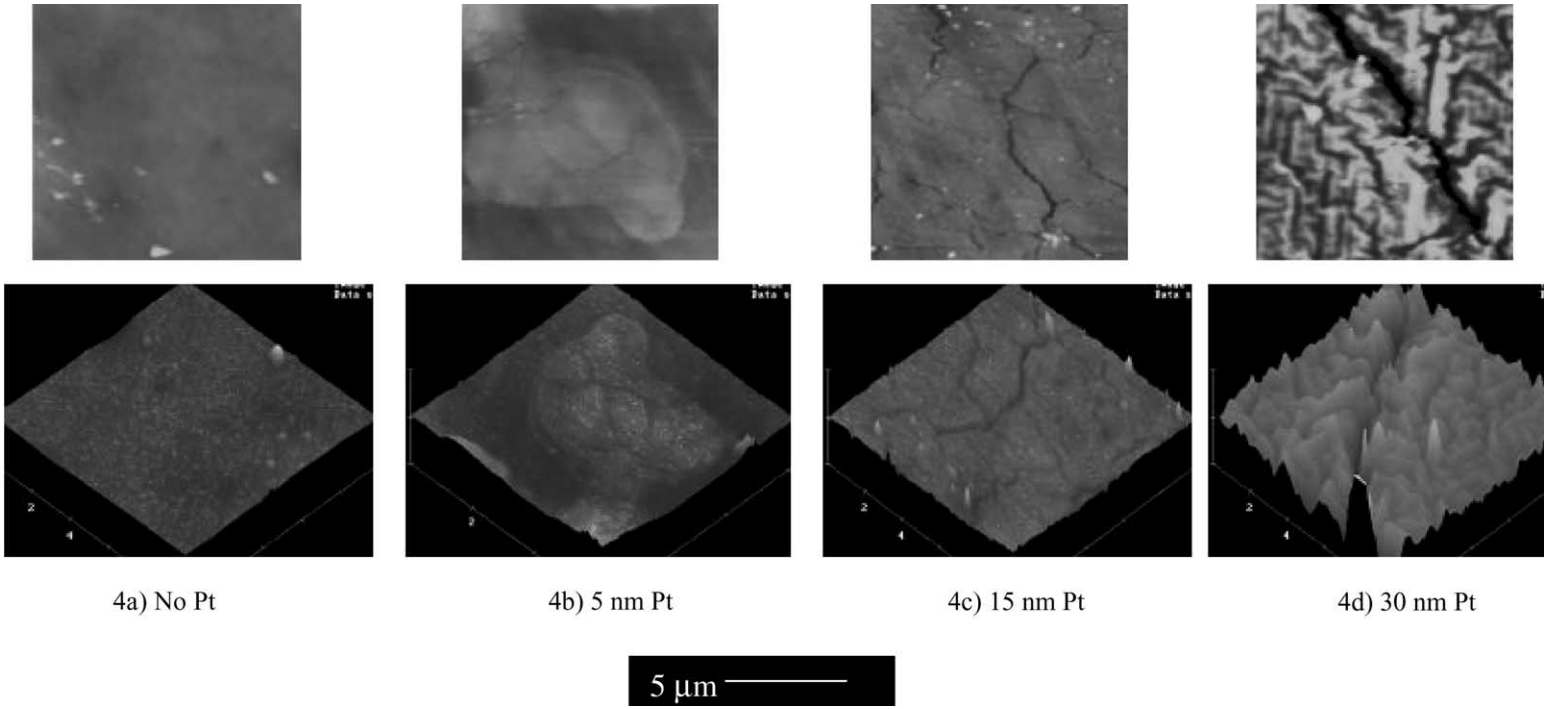

Fig. 3. A series of AFM images (both top and 3D views) showing the morphological evolution of thin platinum films deposited on smooth Nafion 117 as a function of film thickness: (a) bare Nafion 117 surface, (b) A 5 nm thick sputtered platinum film on Nafion 117, (c) A 15 nm thick sputtered platinum film on Nafion 117, (d) A 30 nm thick sputtered platinum film on Nafion 117. All AFM images show a 10 μm × 10 μm square region; the surface relief is shown with a 200 nm data scale in all images.

nanometer level could impact fuel cell performance so dramatically, a microscopy investigation of the thin sputtered platinum films was undertaken.

AFM images were taken of sputtered samples ranging in thickness from 0 nm platinum (bare Nafion), to 30 nm platinum. The AFM results are summarized in Fig. 3. It documents the overall trend towards a coarsening of the platinum film microstructure with increasing film thickness. The bare Nafion surface is quite smooth and relatively featureless (Fig. 3a). At a sputtered thickness of 2 nm (not shown) the surface is still largely unchanged, with only a slight increase in the rms roughness. At 5 nm, scattered domains of platinum (some with fine cracking evident) appear across the surface. These domains are isolated and do not appear to cover the whole surface area. One such domain, exhibiting fine cracking, is shown in the Fig. 3b. By the time the film thickness reaches 15 nm, the cracking behavior is widespread and envelops the whole surface. The cracks are relatively fine, about 0.1 μm wide, and spaced on average 1–2 μm apart (Fig. 3c). At a film thickness of 30 nm, the crack structure is remarkably coarsened. Significant surface texturing is evident, the cracks yawn open approximately 1–2 μm wide, and they are now spaced on average 20–40 μm apart (Fig. 3d). It is believed that the cracking of the platinum film is caused by the water uptake [14] and consequent swelling that occurs when the membranes are removed from the vacuum chamber and exposed to ambient air. Fewer cracks occur in the thicker platinum films due to the increased constraint effects of a thicker metal film on the compliant Nafion substrate.

Additional optical microscope imaging of this coarsening phenomenon is given in Fig. 4. Here, a zoomed out perspective is shown for platinum films of thickness 15, 30, and 100 nm, respectively. As in the AFM images, the coarsening trend is borne out.

The trend towards a coarser film microstructure can help explain the apparent decrease in active platinum area with increasing thickness seen by the CV study of the sputtered films. Increasing thickness decreases the amount of active platinum area in several ways. First, because sputter deposition typically achieves a highly dense and uniform film, the film can quickly cut off reactant gas access to the membrane–catalyst interface as it is made thicker. Thus, for the thicker films, this leaves only the crack sites as regions of legitimate three-phase zone. Additionally, the increasing depth of the cracks with increasing film thickness reduces gas access even to these remaining active catalyst sites. Finally, as can be visually corroborated from the microscopy images, the crack density decreases with increasing film thickness. This leads to fewer available crack site three-phase zones as the film is made thicker, thus further diminishing catalytic activity.

The initial spike in catalyst active area from 2 to 5 nm could be explained with an island coalescence model for the initial growth of the platinum thin film. The island coalescence model is often used to describe the initial growth of sputtered platinum films and has been investigated by several researchers [15,16]. Another group at Stanford University has investigated the growth morphology of ultra-thin (0–5 nm) platinum films sputtered onto glass substrates [17]. Their TEM results reveal nucleation of individual islands of platinum on the SiO_2 substrate with island coalescence occurring at a nominal film thickness of about 2 nm. At this thickness, the platinum islands form a continuous network on the surface. Island coalescence and continuous network formation is essential for good CV testing (and fuel cell performance) as an electrically continuous path is needed in order to harvest the charge generated by active platinum catalyst sites.

While these results are for platinum growth on SiO_2, it can be argued that a similar type of growth phenomenon occurs

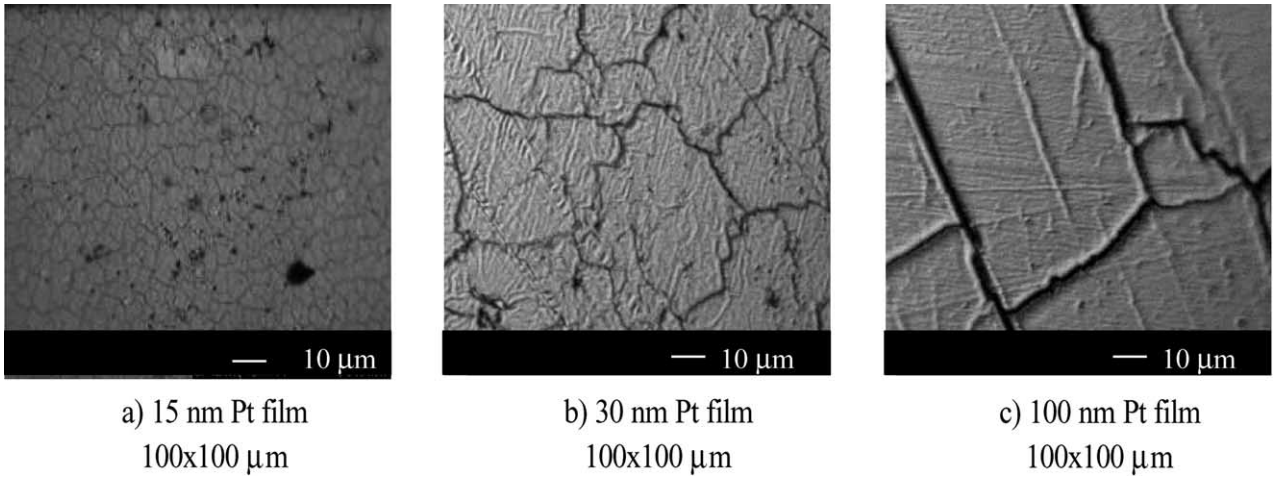

Fig. 4. A series of optical microscope images showing the morphological evolution of thin platinum films deposited on smooth Nafion 117 as a function of film thickness: (a) A 15 nm thick sputtered platinum film on Nafion 117, (b) A 30 nm thick sputtered platinum film on Nafion 117, (c) A 100 nm thick sputtered platinum film on Nafion 117. The optical microscope images are of 100 μm × 100 μm regions, 10 times larger than the AFM images in Fig. 3.

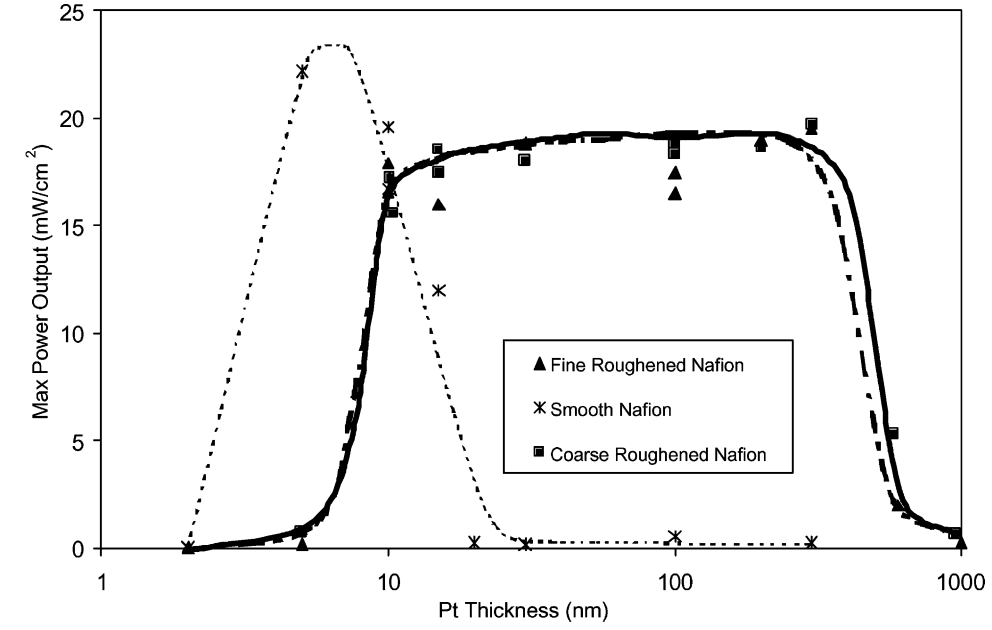

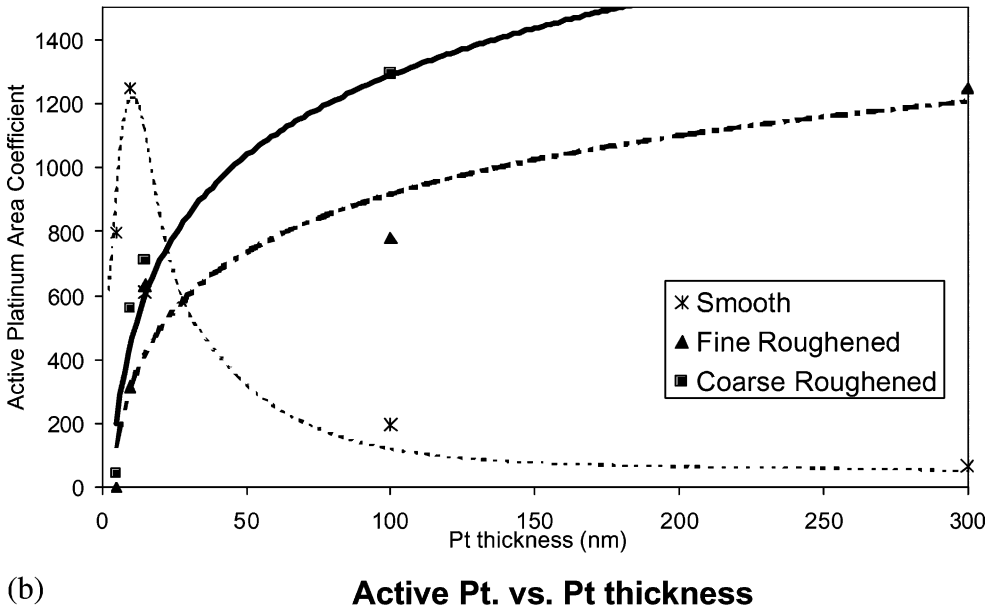

Fig. 5. (a) Fuel cell performance vs. platinum thickness for roughened Nafion 117 sputter-coated membranes: (■) coarse roughened Nafion, (▲) fine roughened Nafion; (b) active platinum area vs. platinum thickness for roughened Nafion 117 sputter-coated membranes: (■) coarse roughened Nafion, (▲) fine roughened Nafion. The smooth Nafion data from Fig. 2 is also shown for reference as the fine dashed line and (∗) symbols. Electrochemical measurements were taken at room temperature using dry (non-humidified) H_2/O_2 at 1 atm.

in platinum films deposited onto Nafion. Furthermore, the higher surface roughness and differing wetting characteristics of Nafion compared to SiO_2 may conspire to delay the onset of island coalescence until a nominal film thickness of 3–4 nm is reached, precisely where the dramatic increase in electrochemically active area and fuel cell performance is seen.

3.3. The effect of intentional surface roughening on fuel cell performance

The intimate correlation between catalyst activity and fuel cell performance suggested that the thin film fuel cells were limited by activation kinetics. Therefore, intentional roughening of the membrane surface was studied as a

method to increase the catalyst active area. Two degrees of roughening were examined: coarse (400-grit SiC abrasion) and fine (600-grit SiC abrasion).

In Fig. 5a, the performances of the roughened Nafion membranes catalyzed by sputter-deposited platinum are charted versus platinum film thickness. The previous results for smooth Nafion are included for comparison. The *x*-axis scale is now logarithmic. Note that the roughened Nafion cells show a broad performance plateau instead of a sharp peak. Performance remains largely constant for over an order of magnitude in platinum film thickness, from 10 to 300 nm. An interesting characteristic of this performance plateau is that it is shifted compared to the smooth Nafion performance peak to higher platinum thickness levels. This behavior suggests that the cells have encountered a new limitation unrelated to catalyst activity, a conclusion that is further corroborated by the CV data given in Fig. 5b. The CV data shows that catalyst activity continues to increase as the films are made thicker, even though fuel cell performance does not. Furthermore, although the effect of coarse roughening shows up in the CV data as an increase in active catalyst area, this also has no impact on fuel cell performance. The fact that increased catalyst area does not translate into increased fuel cell performance suggests that some other limitation is now at work.

There is evidence that ohmic limitations cause the plateau in roughened Nafion MEA performance. Considering that the thin film-sputtered membranes lack hot-pressed electrodes for current collection, contact and current collection resistance losses are significant. High frequency EIS investigations reveal that typical ohmic resistances of the sputtered thin film cells are 2–4 $\Omega\,cm^2$. Even at room temperature in dehydrating conditions, the membrane exhibits a resistance of 0.1 $\Omega\,cm^2$ or less. The sum of the measurement leads and cell fixture resistances were determined to be less than 0.05 Ω. Therefore, almost all of the ohmic resistance results from contact resistance between the cell fixture and the sputtered membrane. An understanding of this loss phenomenon suggests an important avenue for future development.

Referring back to Fig. 5b, it can be seen that the CV behavior of the roughened MEAs differs drastically from that of the smooth MEAs. The smooth Nafion MEAs exhibit a dramatic decrease in active platinum area as the films are made thicker than 5 nm. The roughened MEAs do not exhibit this decline because the roughness affects the

Fig. 6. Scanning electron microscope (SEM) image of the coarse roughened Nafion surface. The surface has been coated with approximately 100 nm of platinum to ensure sufficient conductivity for SEM imaging.

catalyst layer continuity. Fig. 6, an SEM close-up of the roughened Nafion surface, shows that the roughened membrane features are quite fine, typically on the order of 1–10 μm. This surface texturing serves to disrupt the platinum film in a similar fashion and length scale as the fine cracking behavior in the 5–10 nm smooth Nafion films. The sharp angles, higher overall surface areas, and 3D shadowing effects in the roughened membranes keep the amount of three-phase zone high. These extreme surface features allow the membranes to retain roughly the same, if not greater amount of three-phase zone as the platinum is sputtered thicker.

The lack of a thick, continuous film also prevents reactant gas blocking from occurring. This effect can be seen from the EIS data presented in Fig. 7. The 100 nm thick platinum film on smooth Nafion produces both a high frequency activation kinetics loop and a low frequency mass transfer loop, indicating film blocking. However, the 100 nm thick platinum film on roughened Nafion shows only the activation kinetics loop. Another effect of roughened topology is that sufficient electrical continuity cannot be obtained until a thicker film is deposited compared to the films sputtered on smooth Nafion. This delays the onset of good fuel cell performance to thicker film levels, which correlates well with the experimental observations.

3.4. Comparison with conventional MEA technology

It is interesting to compare the results of these platinum thin film fuel cells to the results of PEM fuel cells employing traditional gas diffusion electrode technology. These conventional MEAs typically incorporate a carbon supported platinum catalyst powder mixed with Nafion solution and other solvents to form an ink. This ink is then coated onto a Nafion membrane, which is subsequently hot-pressed with porous carbon cloth or carbon paper electrodes [18–20]. One such conventional MEA was purchased from ElectroChem Inc., with an active area of 5 cm^2 and a catalyst loading of 0.4 mg/cm^2 on Nafion 115. The polarization of this commercial MEA was measured in the same testing fixture as the thin film platinum cells and subject to same test conditions and protocols. A thin film-sputtered platinum MEA was also prepared and tested using smooth Nafion 115 in order to achieve a fair comparison. This membrane was sputtered with approximately 15 nm of platinum on each side using improved and optimized sputter conditions. The platinum loading level of the membrane was approximately 0.04 mg/cm^2. This platinum thickness was optimal for the Nafion 115 membranes, which had a slightly rougher natural surface than the Nafion 117. The performances of the two MEAs are compared in Fig. 8. The conventional MEA produced a

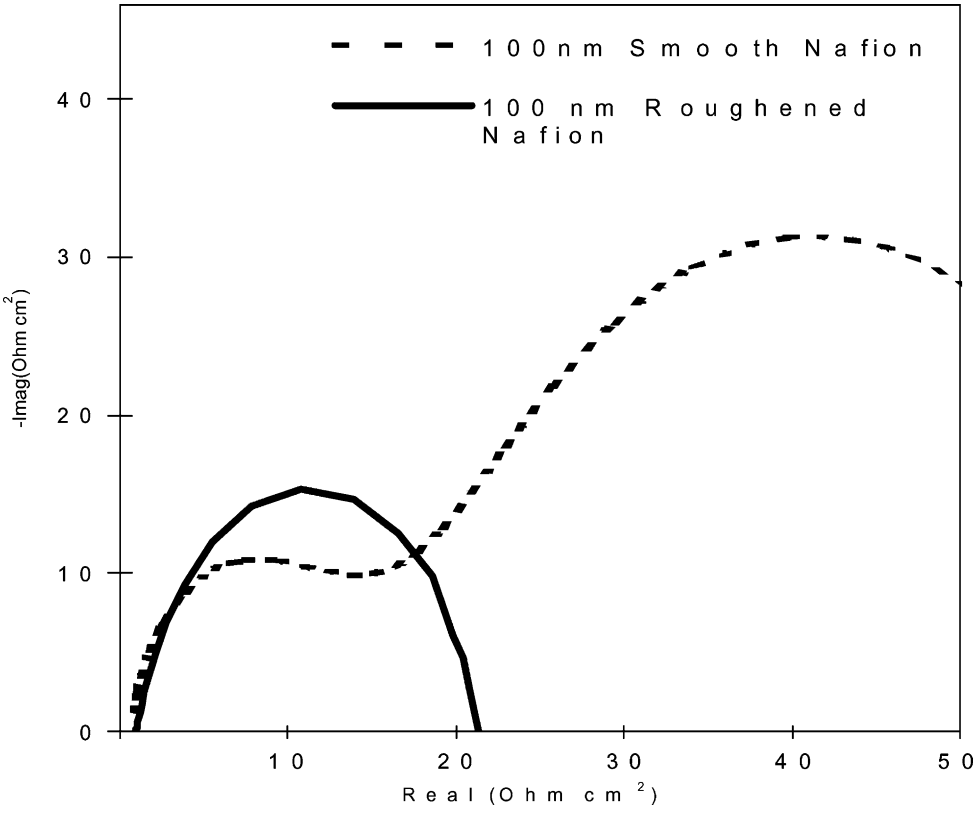

Fig. 7. Measured ac impedance spectra for Nafion 117 sputter-coated membrane fuel cells. A 100 nm thick film on smooth Nafion 117 induces a large mass transfer loop in the impedance spectrum due to reactant gas blockage. Surface roughening of the Nafion 117 prior to catalyst deposition eliminates the mass transfer impedance. Impedance measurements were taken at room temperature using dry (non-humidified) H_2/O_2 at 1 atm.

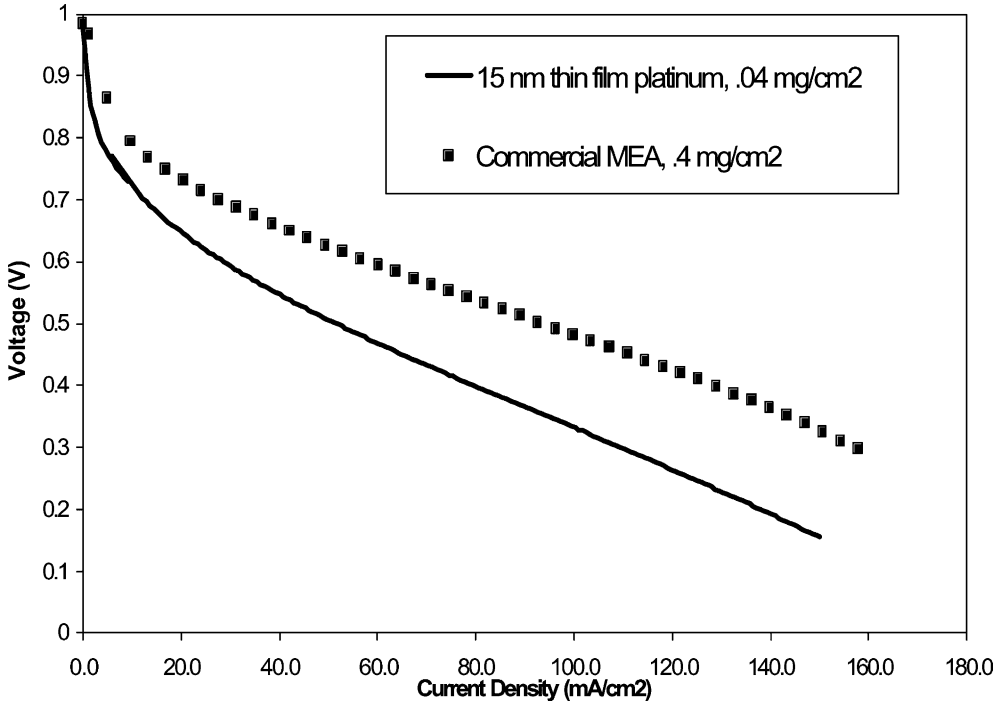

Fig. 8. *I–V* curves comparing the performance of a commercial MEA with 0.4 mg/cm^2 platinum loading to that of a thin film-sputtered platinum MEA with 0.04 mg/cm^2 platinum loading. Cell measurements were taken at room temperature using dry (non-humidified) H_2/O_2 at 1 atm.

maximum power output of 50 mW/cm^2. The thin film MEA produced a maximum power output of 33 mW/cm^2. The higher current density regions of these two curves show similar slopes, indicating that the ohmic resistances in both cells are similar. The difference in performance stems from the higher activation losses in the thin film cell, indicating that the low platinum loading does have an effect on performance. Notably, however, the thin film-sputtered cell attains three-fifths the power density of the commercial MEA with one-tenth of the platinum loading.

4. Conclusions

Under the passive conditions used, it is remarkable how well the thin film MEAs perform compared to the conventional technology. However, it is not safe to assume that their relative performances would remain the same under a different set of conditions. High temperature/fully humidified studies of the thin film cells under optimum conditions should be pursued. The lack of water management ability in the thin film cells might hamper their high temperature/high load performance. On the other hand, the ultra-thin active layer may eliminate mass transfer loss. In addition, improved performance could arise from further investigation of membrane pre-treatment and sputter deposition conditions.

Periodic testing over a 6-month interval revealed no performance degradation. However, degradation issues still merit study, as the effects of continuous long-term or cyclic operation are still unknown. Quantitative measurements of the thin platinum film adherence were not conducted. However, qualitative studies, using a variety of adhesive tapes and scratch-tips indicate that the thin sputtered platinum films adhere strongly to Nafion. For films less than 1000 nm in thickness, film integrity was preserved through a series of water immersions cycles, scratch-tests, and adhesive tape peels. One instance of film delamination was observed in a sample with 1000 nm of sputtered platinum on smooth Nafion. Film integrity is largely a function of the sputtered film—Nafion interfacial properties. Special consideration to the Nafion pre-treatment and cleaning procedures prior to sputter deposition results in strong interfacial adherence.

It has been shown that fuel cell performance is extremely sensitive to sputtered platinum thickness and membrane texture. For smooth Nafion 117 membranes, peak performance is achieved with a sputtered platinum film thickness of 5 nm. This corresponds to a platinum loading level of 0.014 mg/cm^2. Performance decreases significantly for thicker or thinner platinum films due to changes in the film morphology. Roughened membrane surfaces require increased platinum loading levels in order to achieve good performance, but performance is stable over a wide range of thickness values. The merit of membrane roughening is doubtful because it requires increased catalyst loading but does not improve performance.

Ohmic limitations across the thin catalyst film and across the catalyst–current collector interface suggest new design directions. One future goal is the design of a sputter depositable thin film current collector to complement the sputter-deposited catalyst layer. Such an electrode must leave most

of the membrane surface open for reactant gas access while still allowing for efficient, low-loss current collection. Possible manifestations include micro-patterned grid or comb-like geometries, porous thin films, or self-assembling nano-structured electrodes. The benefits of such electrodes over carbon powder include a more intimate electrical contact to the catalyst layer and improved mechanical coherence with the membrane.

Acknowledgements

The authors would like to acknowledge financial support of this work by Honda R&D Co. Ltd. This material is based upon work supported under a Stanford Graduate Fellowship.

References

[1] S. Srinivasan, J. Electrochem. Soc. 136 (1989) 41C.
[2] K.B. Prater, J. Power Sources 51 (1994) 129.
[3] K. Kordesch, G. Simader, Fuel Cells and Their Applications, VCH, Germany, 1996, p. 73.
[4] K.R. Williams, G.T. Burstein, Catal. Today 38 (1997) 401.
[5] S. Hirano, J. Kim, S. Srinivasan, Electrochim. Acta 42 (1997) 1587.
[6] S.Y. Cha, W.M. Lee, J. Electrochem. Soc. 146 (1999) 4055.
[7] C.K. Witham, W. Chun, T.I. Valdez, S.R. Narayanan, Electrochem. Solid State Lett. 3 (2000) 497.
[8] S.J. Lee, S.W. Cha, Y.C. Liu, R.O'Hayre, F.B. Prinz, in: K. Zaghib, S. Surampudi (Eds.), Micro Power Sources, PV 2000-3, The Electrochemical Society Proceeding Series, Pennington, NJ, 2000.
[9] M.S. Wilson, S. Gottesfield, J. Electrochem. Soc. 139 (1992) L28.
[10] S.Y. Cha, W.M. Lee, J. Electrochem. Soc. 146 (1999) 4055.
[11] US Patent No. 4,272,353.
[12] W.C. Choi, J.D. Kim, S.I. Woo, J. Power Sources 96 (2001) 411.
[13] S.A. Sheppard, S.A. Campbell, J.R. Smith, G.W. Lloyd, T.R. Ralph, F.C. Walsh, Analyst 123 (1998) 1923.
[14] T.A. Zawodzinski, C. Derouin, S. Radizinski, R.J. Sherman, V.T. Smith, T.E. Springer, S. Gottesfield, J. Electrochem. Soc. 140 (1993) 1041.
[15] J.A. Venables, G.D.T. Spieler, M. Hanbucken, Rep. Prog. Phys. 47 (1984) 399.
[16] D.E. Savage, F. Liu, V. Zielasek, M.G. Lagally, Semiconductors Semi-Metals 56 (1999) 49.
[17] M.A. Phillips, V. Ramaswamy, B.M. Clemens, W.D. Nix, J. Mater. Res. 15 (2000) 2540.
[18] M.S. Wilson, S. Gottesfield, J. Electrochem. Soc. 139 (1992) L28.
[19] S.J. Lee, Electrochim. Acta 43 (1998) 3693.
[20] C.K. Subramaniam, N. Rajalakshmi, K. Ramya, K.S. Dhathathreyan, Bull. Electrochem. 16 (2000) 350.